Supporting Information

Sun et al. 10.1073/pnas.1018604108

SI Text

Additional Discussion on Spin Order in the CE and Bi-Stripe Phases. Although the main focus of this paper has been the effect of the orbital and charge ordering on the electronic structure, we do also see effects of the spin order on the electronic structure, which we discuss in more detail here. In the CE phase ($x \sim 0.50$), the spins can exhibit either antiferromagnetism ($T < 130$ K) or paramagnetism ($T > 130$ K) (6), as illustrated in Fig. S1. According to double-exchange theory, the ferromagnetic order along the zigzag chains as indicated in Fig. S1*A* should enhance the mobility and metallicity of the hopping electrons. A comparison of the data of Fig. 2 *F* and *G* of the main paper shows this effect, which is noticeable. A more quantitative result is shown in Fig. S1*C*, which is the angle-integrated spectral weight of a dispersive band taken near the zone boundary. It is evident that the evolution of spectral weight with temperature bears a break between 125 K $< T <$ 150 K, which is consistent with the transition temperature, $T \sim 130$ K, of spin structure. However, this behavior is not nearly as strong as the effect of changing temperature in the bi-stripe phase (Fig. 2 *D* and *E*)—for example Fig. 2*G* shows that the Bloch-like E vs. k dispersion persists in the CE samples even when the spin arrangement becomes paramagnetic, indicating that the influence of spin order on the Bloch electronic states is not as strong as the effect of the charge and orbital order. This comparison is also consistent with the fact that the change of conductivity due to the spin valve effect is almost always smaller than unity, while the effect on the conductivity due to the bi-stripes is about five orders of magnitude (7).

As to the spin order in the bi-stripe phase, such information is currently unavailable, though in our higher temperature ($T > 160$ K) measurements it is likely to be paramagnetic. In light of the above discussion of the spin order in the CE phase, the influence of the spin order on the electronic states in the bi-stripe samples is likely to be a smaller secondary effect.

Temperature Dependence of Spectral Weight in the Zone Diagonal Direction. Here we show the equivalent spectra of Fig. 3 in the main paper, except along the nodal cut. In particular, Fig. S2 shows how the spectral weight varies with temperature in the zone diagonal direction of the $x = 0.59$ samples. Along the red cut in Fig. S2*A*, we observe a dispersive band at $T = 20$ K as shown in Fig. 2*C* and reproduced in Fig. S2*B*. In Fig. S2 *C*–*E* we show the variation of spectral weight as a function of temperature, taken along cuts 1–3 in box *B*, respectively. One can notice that the temperature-dependent behavior of the spectral weight is similar to the spectral weight near the zone boundary as shown in Fig. 3.

Band Structure as a Function of Temperature. In addition to the spectral weight transfer out of the dispersive Bloch-like states as the temperature is raised, the overall dispersion of these Bloch-like states varies slightly with temperature as well. This dispersion can best be measured by studying the zone center states which are the farthest from the Fermi energy E_F. Fig. S3*A* shows the position (diamond symbols) of the $d_{x^2-y^2}$ band bottom at $(2\pi,2\pi)$ (equivalent to the zone center but in the second zone), with a nondispersive weight subtracted. We see that the bottom of the band of $d_{x^2-y^2}$ states moves towards the Fermi level with increasing temperature, indicating a decrease in the bandwidth $W/2$ (gold diamonds in Fig. 4, also see *Additional Discussion on Underlying Physics* for more discussion on the bandwidth). This decrease in bandwidth is qualitatively consistent with a double-exchange-induced reduction in hopping amplitude due to increasing spin disorder at high temperatures (1, 2). However, as we found for $x = 0.40$ compounds, the reduction in bandwidth is smaller than what would be expected for the reduction in the sample's magnetization (3)—a behavior requiring further investigation. Fig. S3*B* shows the temperature dependence of the states at the $(\pi,0)$ point. This data is obtained by subtracting EDC cut 3 from EDC cut 1 of Fig. 3 *A* and *C*. All "differential" curves are stacked for comparison, and one can notice that, in addition to the loss of the spectral weight, the bottom of the dispersive $d_{x^2-y^2}$ band moves to slightly deeper binding energies with increasing temperature. The shift of the band bottom begins to occur far below T_c. The systematic changes are summarized in Fig. S3*C*.

Additional Discussion on Underlying Physics. A tight-binding type picture with stripe localization and no additional interactions would place the localized electronic weight at the mean of the energies of the band. Because the band is approximately half (60% holes) full, this would be an energy very near the Fermi energy, while the experiment shows that these states appear at an energy approximately −0.8 eV. Therefore, additional physics such as Coulomb interactions (Mott physics) or small polaronic interactions must be at play. Within the Mott picture the extra 0.8 eV would come from on-site Coulomb interactions, while within the small polaron picture this would be the extra binding energy that the localized electrons gain from a local lattice distortion. A critical point here is that these interactions (Mott or small polaronic) are not on their own able to drive the system insulating—they instead depend upon the stripes to do the major portion of the work. That this point is true can be seen by comparing the relevant energy scales. For a doping of ∼60%, approximately half of the band is above E_F, so the full bandwidth W should be ∼3 eV. This estimate is also supported by band calculations (4). Similarly, the upper Hubbard band is expected to be $\sim U/2$ above E_F, with $U/2 \sim 0.8$ eV. These scales indicate that the U is significantly less than the bandwidth W, while for a Mott transition without the help of the stripe localization we should have a decreasing bandwidth W as T_c is approached, such that $U \sim W$ at the Mott transition. Similar energy scale arguments would follow for a polaron-driven transition, or a transition involving the cooperation between polaronic and Mott physics. In contrast, our data does not show a significant reduction in the bandwidth of the dispersive states as T_c is approached, (gold diamonds in Fig. 4) implying that these Bloch-like portions of the states are not feeling significant Mott or polaronic correlations. On the other hand, once the stripes have initially localized the electrons, the bandwidth of these localized electrons is driven toward zero, implying that U/W for these already-localized states is now $\gg 1$ and Mott or polaron physics can now enter the problem. Without the bi-stripe localization the Mott or polaronic physics is not able to play a significant role.

Stoichiometric Inhomogeneity. In correlated electronic systems, stoichiometric inhomogeneity is sometimes an important issue, and one may wonder about its contribution here. In particular, we consider whether local $x = 0.60$ patches in the $x \sim 0.59$ host material could give rise to the "residual" localized electronic states which are part of the evidence for fluctuating stripes. For example, Beale et al. reported residual static bi-stripe components at low temperatures, which however give rise to minimal scattering signals three orders of magnitude smaller than the high temperature measurements at ∼200 K (5). Generally speaking, such small components should be invisible in our angle-resolved

photoemission spectroscopy (ARPES) data. On the other hand, from the temperature dependence of the localized (or nondispersive) weight (Fig. 2 *D* and *E*) we notice that a remarkable amount of localized weight varies strongly with temperature, even flattening off at the 160 K transition temperature of the bulk material (black circles in Fig. 4), which cannot be accounted for by the residual bi-stripe components at low temperatures.

1. Zener C (1951) Interaction between the *d*-shells in the transition metals. II. Ferromagnetic compounds of manganese with perovskite structure. *Phys Rev* 82:403–405.
2. Anderson PW, Hasegawa H (1955) Considerations on double-exchange. *Phys Rev* 100:675–681.
3. Saitoh T, et al. (2000) Temperature-dependent pseudogaps in colossal magnetoresistive oxides. *Phys Rev B* 62:1039–1043.
4. Sun Z, et al. (2008) Electronic structure of the metallic ground state of $La_{2-2x}Sr_{1+2x}Mn_2O_7$ for $x \sim 0.59$ and comparison with $x = 0.36$, 0.38 compounds as revealed by angle-resolved photoemission. *Phys Rev B* 78:075101.
5. Beale TAW, et al. (2005) Orbital bi-stripes in highly doped bilayer manganites. *Phys Rev B* 72:064432.
6. Li QA, et al. (2007) Reentrant orbital order and the true ground state of $LaSr_2Mn_2O_7$. *Phys Rev Lett* 98:167201.
7. Li QA, et al. (2006) First-order metal-insulator transitions in manganites: are they universal? *Phys Rev Lett* 96:087201.

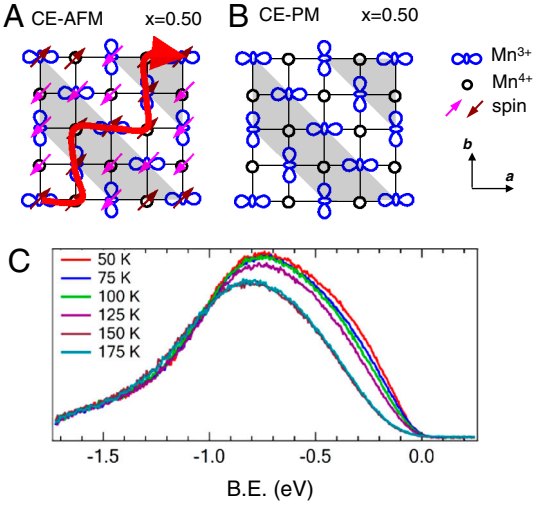

Fig. S1. (*A*) CE phase with antiferromagnetic spin order. (*B*) CE phase with paramagnetic spin order. The red path indicates a possible hopping path for mobile electrons with a ferromagnetic spin order. (*C*) Integrated spectral weight of a dispersive band taken near the zone boundary from $La_{2-2x}Sr_{1+2x}Mn_2O_7$ ($x = 0.50$).

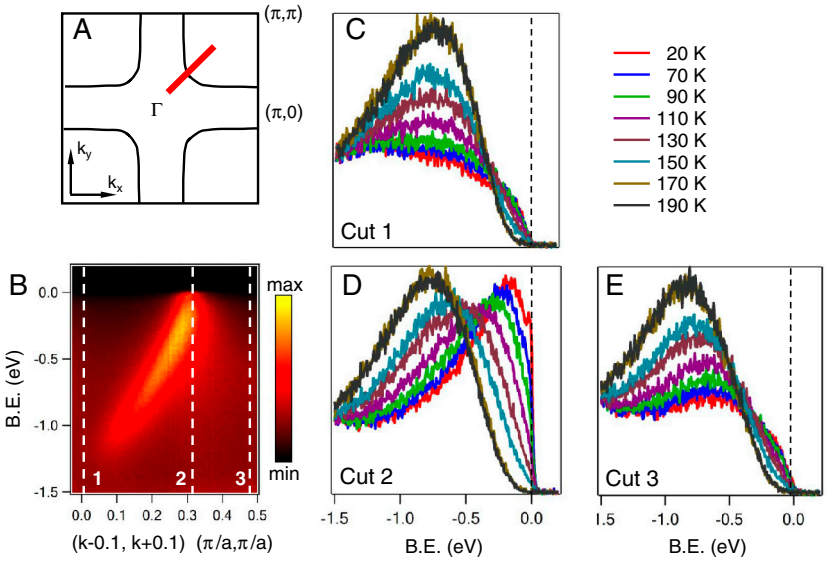

Fig. S2. Temperature dependence of the electronic structure of $x = 0.59$ samples in the nodal direction. (*A*) A schematic Fermi surface plot. (*B*) Energy vs. momentum dispersive band taken at $T \sim 20$ K along the red cut in box *A*. (*C*, *D*, *E*) Temperature dependence of EDC cuts 1, 2, and 3, indicated by the white dashed lines in box *B*, taken at various temperatures.

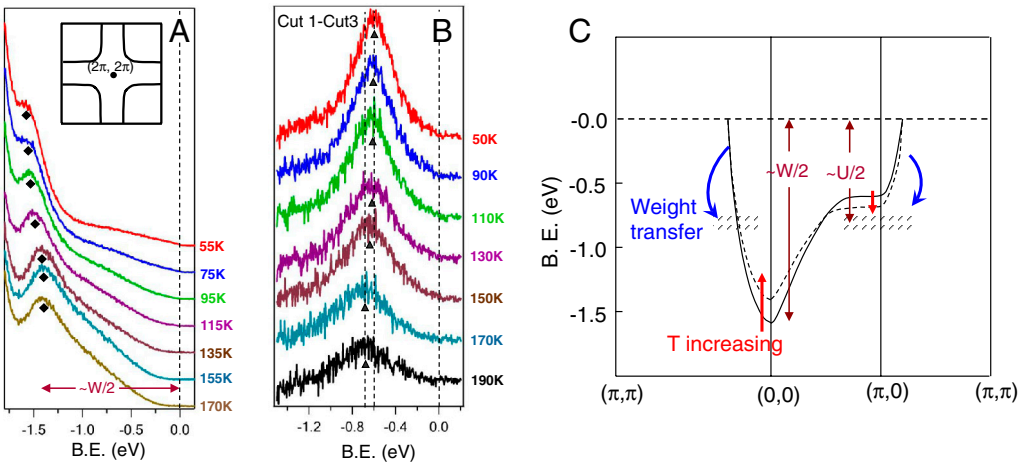

Fig. S3. (*A*) EDCs of $x = 0.59$ $La_{2-2x}Sr_{1+2x}Mn_2O_7$ taken at the band bottom $(2\pi,2\pi)$ at various temperatures, with a background subtracted to make the band bottom more visible. (*B*) Differential EDCs at the $(\pi,0)$ point obtained by subtracting EDC cut 3 from EDC cut 1. (*C*) Schematic plot of the change of the dispersion of the $d_{x^2-y^2}$ band and the weight transfer from the dispersive $d_{x^2-y^2}$ band to the nondispersive feature (hatched area) with increasing temperature.